OpenAccess

Atomistic simulation of CeO_2 surface hydroxylation: implications for glass polishing

Christopher R. Stanek · Averyl H. H. Tan ·
Scott L. Owens · Robin W. Grimes

Abstract Atomistic simulation techniques have been used to investigate the dissociative adsorption of water on the (110), (111), and (100) low index surfaces of CeO_2, as well as a so-called "trench" surface configuration. Several different coverages of water have been considered to better understand how the hydroxylation process progresses. Hydroxylation energies and surface energies of CeO_2 calculated via atomistic simulations are compared to similar results for other fluorite oxides. Finally, the modification of CeO_2 crystallite morphology in the presence of water is predicted from the changes in surface energy and the implications of these morphological changes for glass polishing are discussed.

Introduction

CeO_2 is used in a variety of industrial applications, such as in oxidation catalysis, solid oxide fuel cells, and glass polishing. In many applications (including those mentioned), processes occurring at the surfaces govern CeO_2 functionality. For this reason, it would be beneficial to better understand the surface properties of CeO_2. Although

C. R. Stanek
Material Science and Technology Division, Los Alamos
National Laboratory, Los Alamos, NM 87545, USA

A. H. H. Tan · R. W. Grimes (✉)
Department of Materials, Imperial College, London SW7 2BP,
UK
e-mail: r.grimes@imperial.ac.uk

S. L. Owens
Nexia Solutions Ltd., Warrington, Cheshire WA3 6AS, UK

many studies have addressed CeO_2 surface structure and related properties (e.g., [1–4]), relatively few have been concerned with CeO_2 surfaces in the presence of water. This is particularly significant to the application of glass polishing because the efficacy of CeO_2 abrasive particles depends upon the morphology (or "shape"), which is governed by the relative surface energies of those particles while in the presence of water [5, 6].

The mechanism by which glass is polished has been debated for at least 350 years (see [7] and [8] for a more complete description). Despite a long history, it is still the case that no one theory for the mechanism of glass polishing is unequivocally accepted. Rather, three discrete classifications of theory have emerged. Hooke [9], Newton [10], and Rayleigh [11] were all proponents of the so-called "*wear theory*," which explains glass polishing through the mechanical removal of material by an abrasive polishing agent, and in its simplest terms, is an extension of grinding. Beilby proposed an alternative mechanism [12, 13], known as the "*flow theory*," where the polishing agent forms an amorphous glass layer that can be smeared to fill voids in the glass surface. Finally, Preston [14] and Grebenshchikov [15] advanced the "*chemical theory*," which points to the chemical reactions between the polishing agent and the glass surface as the critical component of the polishing process. It is likely that each of these theories play a role in the polishing process, and a generalized "mechano-chemical" mechanism is now nominally accepted [16, 17]. What remains to be established, however, is whether *chemical* or *mechanical* effects dominate.

Only few compounds effectively polish glass, and CeO_2 is one of the best [18, 19]. Interestingly, isostructural ZrO_2 has a polishing rate less than half of CeO_2 [19]. The maximum polishing activity of CeO_2 is achieved by crushing particles sintered at approximately 900 °C [7].

The given reason for this observation is that this sintering temperature yields finer particles which are able to more frequently interact with the glass surface, but it is not so high that the particles sinter together. (*Note*: Newton also proposed that small particles were more effective at polishing glass, but for the reason that they make smaller scratches on the surface [10]). The optimum preparation route for CeO_2 (according to Izumitani [7]) is one that results in a material that is harder than the glass to be polished, but soft enough to be crushed during polishing.

The hardness of the polishing agent is certainly important, but it alone does not completely explain the pronounced efficacy of CeO_2. Thus, it has been suggested that chemical reactions between CeO_2 and the glass surface also play a role [14, 15]. Recently, it has been established that the not only the size, but also the shape of the CeO_2 crystallites may control the polishing rate [5]. This observation led to subsequent investigations on the effect of synthesis processing on the morphology of CeO_2 crystallites [6]. These studies revealed that a more regular distribution of polishing agent particle sizes and morphologies led to more efficient polishing. However, the starting morphology of a CeO_2 crystallite should not be expected to remain constant during the polishing process, especially in the presence of water. Furthermore, a morphology of CeO_2 crystallites dominated by (111) facets has been proposed as the optimum shape [5, 6], but it is not entirely clear why this is so.

In this study, we use atomistic simulation to predict the energy associated with the dissociation of water on the (100), (110), and (111) low index surfaces of CeO_2. Consequently, those surfaces which are more strongly stabilized by the presence of hydroxide will be identified. This provides a connection between dissociation of water and particle morphology. Furthermore, based on these results we are able to provide some comments that relate the role of particle morphology to the efficacy of glass polishing.

Previous CeO_2 surface simulation studies

Sayle et al. [20] used similar interatomic potential simulation techniques to those employed in this article to model the surface energies of dry CeO_2. In that study, the Type 1 (110) and (310) surfaces (definition of ionic surface type according to Tasker [21]) as well as the Type 2 (111) surface were considered, while the Type 3 (100) surface was not originally considered [20]. Of these, they found the (111) surface to exhibit the lowest surface energy, followed by the (110) and the (310). Conesa [1] expanded on the work of Sayle et al. [20] and examined the stability of the Type 3 (100) surface. To neutralize this dipolar surface, half of the surface oxygen ions were removed (in a checkerboard type configuration).

Using the same potentials as Sayle et al. [20], Conesa found that based upon energetic considerations, the (100) should not be disregarded. Vyas et al. [3] derived a new set of robust potentials, which were able to reproduce the structures of higher index surfaces (e.g., (331), (411), etc.). This work also began to show how CeO_2 surface energetics translate to a crystallite morphology. Baudin et al. [22] and Gotte et al. [23] subsequently built upon these static simulations to consider the dynamics of CeO_2 surfaces.

Gennard et al. [24] compared results from Hartree-Fock quantum mechanical simulations of bulk and surface properties of CeO_2 (and ZrO_2) to those calculated using interatomic potentials. They found that the energy difference between the (110) and (111) surfaces agreed well with the previous interatomic potential results, though their absolute energies were consistently lower. Skorodumova et al. [4] used density functional theory (both the local density approximation (LDA) and generalized gradient approximation (GGA)) to determine the (111), (110), and (100) surface properties of CeO_2. Although the absolute energies were not consistent (even between LDA and GGA), the relative surface energy stability trends remain the same as calculated by the afore-mentioned methods.

In addition to surface stability, the hydroxylation of surfaces has also been simulated. Redfern et al. [25] used interatomic potentials to simulate the hydroxylation of tetragonal-ZrO_2 surfaces. The primary conclusion of Redfern et al. [25] was that the equilibrium morphology of tetragonal ZrO_2 crystallites is expected to be different in aqueous conditions than in dry conditions. This is because the low-energy surface that dominates this tetragonal crystallite morphology in dry conditions (the (101)) exhibits no tendency to hydroxylate. However, higher energy dry surfaces (e.g., (110)B) exhibit a pronounced tendency to hydroxylate, which then lowers the overall surface energy. The reduction of the (110)B surface energy via hydroxylation increases the stability of this surface so that it is energetically similar to the (101). Similarly, Abramowski et al. [26] and Tan et al. [27] simulated the hydroxylation behavior of UO_2 and PuO_2, respectively, and again predicted that the crystallite morphology of these compounds is different in the presence of water. Finally, Kumar and Schelling recently considered the adsorption of water on the CeO_2 (111) surface via density functional theory [28]. We will compare our results to those of Kumar and Schelling in the "Results" section.

Methodology

To calculate surface energies, the code MARVIN [29] was employed. As outlined in previous studies [26, 29, 30] MARVIN is a 2D periodic boundary code, where the repeat

unit is divided into an upper region I and lower region II. All ions in region I are relaxed using energy minimization while those in region II are held fixed at their perfect lattice positions [29]. As is the case with the total depth of the simulation block, regions I and II are chosen so that further enlargement has a negligible effect on total energies (in this study region I is $3 \times 3 \times 6$ unit cells). MARVIN employs Parry's variant of the Ewald technique [31, 32] to sum long-range electrostatic forces. Short-range interactions are described by the Buckingham potential [33]. The potential parameters for Ce^{4+}–O^{2-} and O^{2-}–O^{2-} can be found in the papers where the original derivation is described ([3] and [34], respectively). Dipoles can be of great significance at surfaces. In addition to the movement of ions, dipoles will also be formed through the displacement of charge around a single ion (i.e., polarization). Here such effects are included by using a core/shell model [35] and the shell parameters are available in the original papers [3, 34].

The methodology described above can be used to calculate two important energies that will characterize the hydroxylation phenomena, namely: surface energy and hydroxylation energy. The surface energy can be defined as

$$\gamma = \frac{E_{surf} - E_{bulk}}{A}, \tag{1}$$

where A is the area of the new surface formed, E_{surf} is the total energy associated with the ions in region I of the 2D repeat unit and E_{bulk} is the total energy associated with the same number of ions in a 3D perfect lattice. This is, therefore, the internal energy to cleave a perfect surface and create a new surface. We define hydroxylation energy as the energy gained per water molecule at a specific coverage of water. The method to calculate hydroxylation energies is described elsewhere [25, 26].

The use of fixed interatomic potentials to study surface hydroxylation is a necessary approximation given the large number of possible configurations and large repeat unit cell sizes that must be used to accurately model this problem. Support for the reliability of the interatomic potentials used in this work comes from the similarity of surface-related properties calculated using potentials of this type and equivalent surface studies that employ quantum mechanical-based methods as well as experimental observation of crystallite morphology. Several modeling studies for CeO_2 were described in the previous section. Another example is the study by Skomurski et al. [36], where the plane wave code CASTEP was used to examine the relative stability of the (111), (110), and (100) surfaces of UO_2 (which is isostructural to CeO_2). Their results agreed favorably with previous results generated with interatomic potentials [30].

Results

The (111), (110), and (100) surface energies of CeO_2 were calculated at 0, 12.5, 25, 50, 75, and 100% hydroxylation. "Hydroxylation" was simulated by positioning an OH^- group directly above a surface cation and associating the remaining H^+ of one water molecule with a surface oxygen. All atom positions are then allowed to relax to their equilibrium positions. Consequently, percent hydroxylation is defined as the number of surface cations (or oxygen atoms) covered by water molecules (see [25] for a thorough discussion).

Three configurations of the anion terminated (100) surface (so-called A, B, and AB) were considered based upon results of previous studies (see [37] for further details). These three configurations, depicted in Fig. 1, are considered since they are of low energy when compared to other unique configurations of the (100) surface [37]). A trench configuration where (111) facets form grooves on the (100) surface in [110] directions has also been considered (see [27, 37] for additional details of the trench structure). The calculated surface energies of each of these surfaces are described in Table 1. As found in previous theoretical studies [1, 4, 20, 24], the lowest energy dry surface was found to be the (111), followed by the (110) and (100) surfaces. However, as these surfaces become hydroxylated, the energy of the (111) surface increases (becomes less favorable) and at approximately 75% water coverage actually becomes greater than the surface energies of the (110) and (100) surfaces.


Fig. 1 Three 3×3 unit cell anion configurations of the CeO_2 (100) surface, where the spheres refer to surface oxygen atoms and the unoccupied squares refer to surface vacancies. The nomenclature for these configurations (i.e., A, B, and AB) is used throughout the text

(a) A config.　　(b) B config.　　(c) AB config.
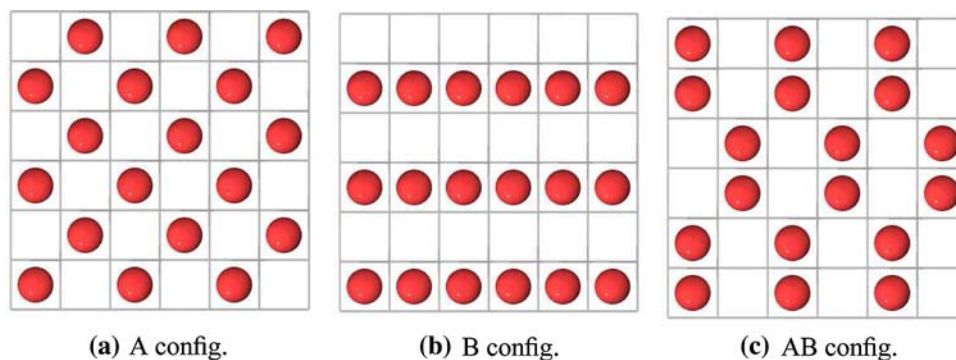
Table 1 Surface energies (J/m^2) of dry and hydroxylated surfaces of CeO$_2$

| % H$_2$O	(111)	(110)	(100)A	(100)B	(100)AB	Trench
0	1.39	2.17	2.94	3.30	2.88	2.56
5.6	–	–	–	–	–	2.44
11.1	–	–	–	–	–	2.33
12.5	1.41	2.05	2.62	2.54	2.60	–
16.7	–	–	–	–	–	2.25
22.2	–	–	–	–	–	2.17
25	1.47	1.94	2.49	2.27	2.42	–
27.8	–	–	–	–	–	2.06
33.3	–	–	–	–	–	2.03
38.9	–	–	–	–	–	2.08
44.4	–	–	–	–	–	2.00
50	1.74	1.80	2.32	2.32	1.88	2.02
55.6	–	–	–	–	–	2.04
61.1	–	–	–	–	–	2.08
66.7	–	–	–	–	–	2.06
72.2	–	–	–	–	–	2.05
75	1.95	1.82	1.86	1.98	1.80	–
77.8	–	–	–	–	–	1.89
83.3	–	–	–	–	–	2.03
88.9	–	–	–	–	–	2.20
94.4	–	–	–	–	–	2.37
100	3.16	1.89	1.93	1.93	1.82	1.91

The implication of the (111) surface energy being greater than the hydroxylated (100) surface energy is that the equilibrium CeO$_2$ crystallite morphology will vary depending on the degree of hydroxylation. Figure 2 shows the predicted morphology of CeO$_2$ under dry and low hydroxylation conditions. This morphology is clearly dominated by (111) faces. However, when increasing hydroxylation sufficiently reduces the (100) surface energy (relative to the (111) surface), (100) facets will appear, as shown in Fig. 3. This is consistent with the observation of
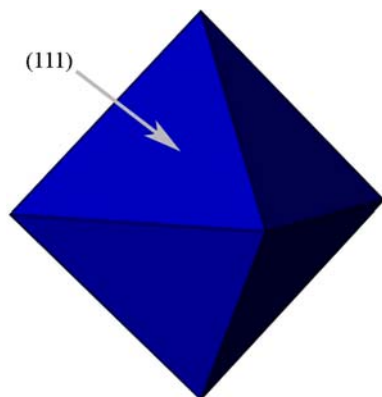
Kirk and Wood [6] who found that the surface area of (100) facets on (111) planes decreased with increasing calcination temperature. Since the CeO$_2$ samples that Kirk and Wood examined were synthesized through a sol–gel process, it is reasonable to expect that water molecules were available for the hydroxylation of surfaces. The reduction in (100) surface area with calcination temperature may suggest that the water molecules stabilizing the (100) surface were removed at the higher temperature. Encouragingly, our prediction of CeO$_2$ morphology in the presence of water (Fig. 3) is nearly identical to the morphology of an approximately 80 nm CeO$_2$ particle observed by Kirk and Wood, after sintering at 850 °C [6].

Calculated hydroxylation energies for the CeO$_2$ surfaces are plotted as a function of water coverage in Fig. 4, where it is assumed that the hydroxylation energy changes approximately linearly between calculated points. It is clear from Fig. 4 that the hydroxylation energy for the (111) surface is initially close to zero, but becomes more positive (i.e., even less favorable) at greater coverages of water. This suggests that the (111) surface does not exhibit a strong driving force to bind hydroxide species to surface sites. These results compared favourably to the results of Kumar and Schelling [28]. In particular, we calculated a hydroxylation energy of 0.55 eV for the (111) surface at 50% hydroxylation, while Kumar and Schelling calculated adsorption energies of 0.56 and 0.58 eV for two different configurations of a 0.5 monolayer of water on the (111) surface. However, it should be noted that this comparison is only favorable if our hydroxylation energy is similar to the adsorption energy of Kumar and Schelling and if 50% hydroxylation corresponds to a 0.5 monolayer.

In contrast to the (111) surface, the (110), (100), and trench surfaces all have negative hydroxylation energies, suggesting that these surfaces will react with available

Fig. 2 The predicted morphology of CeO$_2$ crystallites under dry or low hydroxylation conditions
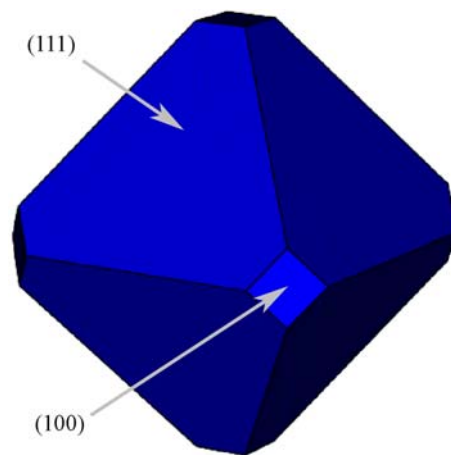
Fig. 3 The predicted morphology of CeO$_2$ crystallites under moderate to high hydroxylation conditions, where the (100) facet surface area is expected to increase as a function of extent of hydroxylation
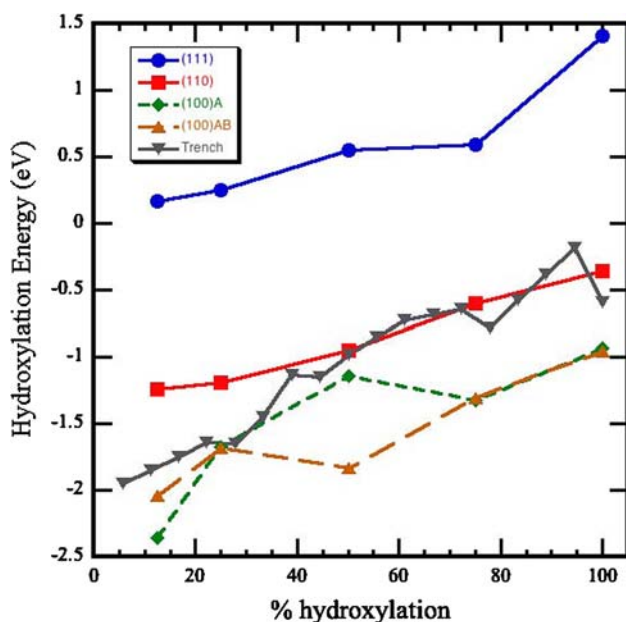
Fig. 4 Comparison of the hydroxylation energies of all CeO_2 surfaces considered in this study. Of particular note, the (111) hydroxylation energy is near to but greater than 0 eV for the entire hydroxylation range

water to form stable hydroxylated structures and that hydroxide species are strongly bound to these surfaces. Qualitatively, these predictions can be understood in terms of surface stability and structure of the dry surfaces. The (111) surface is relatively stable when dry, and it is therefore, difficult for hydroxylation to contribute to further stability of the surface. On the other hand, in order for the anion terminated (100) surface to be stable under dry conditions, half of the surface oxygen ions must be removed to neutralize the dipole normal to the surface [1, 37]. Since the (100) surface has surface sites that can accommodate the oxygen ions of hydroxide species with a high coordination to adjacent cations, it is not unreasonable to expect that the addition of hydroxide (hydroxylation) will lower the surface energy.

Summary

We have shown that the equilibrium morphology of CeO_2 crystallites will be modified in the presence of water. For glass polishing, it has been recently proposed that in addition to the crystallite size of the glass polishing agent, the shape of the crystallite also plays a role in the efficacy of the glass polishing process [6]. To show this, Kirk and Wood evaluated the polishing efficiency of CeO_2 as a function of calcination time and temperature [6]. Izumitani had already shown that the polishing rate of CeO_2 starts to

decrease when the material is sintered above 900 °C. It is possible that a contributing factor as to why there is a decrease in polishing efficiency for material sintered at higher temperatures is simply that individual CeO_2 particles begin to sinter together. Recall, however, that Kirk and Wood found the morphology of CeO_2 crystallites calcined at 325 °C had large (100) facets on (111) planes. When calcined at 850 °C, the surface area of the (100) facets decreased, and the morphology was dominated by (111) faces. Furthermore, this material was found to polish glass rather better, leading Kirk and Wood to conclude that the (111) surface of CeO_2 is more effective at polishing glass than the (100) surface [6]. Kirk and Wood suggested the reason for this was that the (111) surface has more Ce atoms per unit surface (there are 2.31 Ce/a_o^2 for the (100) surface and 2.00 Ce/a_o^2 and 1.41 Ce/a_o^2, respectively, for the (100) and (110) surfaces). This is a plausible explanation if it is the Ce^{4+} ion that is critical to the mechano-chemical process. However, we wish to suggest an alternative possibility. If the chemical process that takes place between CeO_2 and the glass surfaces involves transfer of protons or hydroxide species from the CeO_2 surface to the glass, then the (111) surface would be more effective than either the (100) or (110) surfaces, simply because the (111) surface does not exhibit a strong affinity for hydroxide species. Indeed, it may even be that the (111) surface provides a source of hydroxide or protons by promoting the dissociation of H_2O (i.e., catalytic). Certainly, the transfer of hydroxide and protons to the silica, resulting in mulitple Si–OH bonds will lead to removal of silicate species material from the glass surface because $Si(OH)_4$ is soluble in water. Moreover, this may explain why ZrO_2 is less effective than CeO_2, as the (111) surface of ZrO_2 has a strongly negative hydroxylation energy [38] and as such will not promote the formation of hydroxide species. Finally, the (111) surface of UO_2 also exhibits a clearly negative hydroxylation energy [30], which would be consistent with this material being a less effective polishing agent since the surface will exhibit an energy barrier to the release of a hydroxide or proton. In conclusion, based on the idea that (111) surfaces most readily yield hydroxide or protons that may interact with the glass surface, to maximize the glass polishing efficacy of CeO_2, this material should be synthesized such that the morphology of crystallites is dominated by (111) facets, while maintaining small particle size for large overall surface area.

References

1. Conesa J (1995) Surf Sci 339:337
2. Sayle T, Parker S, Catlow C (1994) Surf Sci 316:329
3. Vyas S, Grimes R, Gay D, Rohl A (1998) J Chem Soc Faraday Trans 94:427
4. Skorodumova N, Baudin M, Hermansson K (2004) Phys Rev B 69:075401
5. Kirk N (1993) Ph.D. thesis, University of Nottingham
6. Kirk N, Wood J (1995) J Mater Sci 30:2171
7. Izumitani T (1988) Optical glass. American Institute of Physics, New York
8. Holland L (1964) The properties of glass surfaces. Chapman and Hall, London
9. Hooke R (1665) Micrographia: or some physiological descriptions of minute bodies made by magnifying glasses with observations and inquiries thereupon. Martyn and Allestry, London
10. Newton I (1704) Opticks: or a treatise of the reflexions, refractions, inflexions and colours of light. Smith and Walford, London
11. Rayleigh J (1901) Nature 64:385
12. Beilby G (1903) Proc Roy Soc A 72:218
13. Beilby G (1921) Aggregation and flow of solids. Macmillan and Co, London
14. Preston F (1930) J Soc Glass Tech 14:127
15. Grebenshchikov I (1931) Keram i Steklo 7:36
16. Cook L (1990) J Non-Cryst Solids 120:152
17. Kirk N, Wood J (1994) Br Ceram Trans 93:25
18. Kaller A (1962) Mschr Feinmech Opt 79
19. Silvernail W, Goetzinger N (1971) Glass Ind 52:130
20. Sayle D, Parker S, Harding J (1994) Philos Mag A 69:787
21. Tasker P (1979) J Phys C 12:4977
22. Baudin M, Wójcik M, Hermansson K (2000) Surf Sci 468:51
23. Gotte A, Hermansson K, Baudin M (2004) Surf Sci 552:273
24. Gennard S, Corà F (1999) J Phys Chem B 103:10158
25. Redfern S, Grimes R, Rawlings R (2001) J Mater Chem 11:449
26. Abramowski M, Redfern S, Grimes R, Owens S (2001) Surf Sci 490:415
27. Tan A, Grimes R, Owens S (2005) J Nucl Mater 344:12
28. Kumar S, Schelling P (2006) J Chem Phys 125:204704
29. Gay D, Rohl A (1995) J Chem Faraday Trans 91:925
30. Abramowski M, Grimes R, Owens S (1999) J Nucl Mater 275:12
31. Parry D (1975) Surf Sci 49:433
32. Parry D (1976) Surf Sci 54:195
33. Buckingham R (1938) Proc Roy Soc A 168:264
34. Binks D, Grimes R (1993) J Am Ceram Soc 76:2370
35. Dick B, Overhauser A (1958) Phys Rev 112:90
36. Skomurski F, Becker U, Ewing R (2004) Geochim Cosmochim Acta 68:A119
37. Tan A, Abramowski M, Grimes R, Owens S (2005) Phys Rev B 72:035457
38. Tan A (2006) Ph.D. thesis Imperial College, London